COOPERATIVE OBSTACLE AVOIDANCE CONTROL OF FIN STABILISER BASED ON ADAPTIVE RBF NEURAL NETWORK

Mingxiao Sun*,** Houxin Lian,* Yongde Zhang,** and Tiantian Luan*,**

Abstract

The safety of the anti-roll fin during operation is the primary factor in ensuring the effectiveness of ship anti-roll, which involves planning the safe movement area of the fin body when the ship encounters marine obstacles. This paper proposes an adaptive RBF neural network-based collaborative obstacle avoidance control method to ensure the safe obstacle avoidance of anti-roll fins without affecting the anti-roll effect. Firstly, the RBF neural network is used to approximate the uncertainty of the roll motion model, design adaptive weights, handle nonlinear and uncertain links, and improve the anti-interference performance of the system. Subsequently, the maximum fin angle for obstacle avoidance is introduced to solve the safe motion area of the fin body. On this basis, considering the constraints of fin motion and the loss of control torque caused by obstacle avoidance, collaborative control of the front and rear fin motion is carried out to compensate for the loss of roll reduction efficiency.

Key Words

Fin stabiliser, adaptive control, RBF neural network, obstacle avoidance, cooperative control

1. Introduction

Due to the complex and ever-changing marine environment, marine navigation is susceptible to interference, resulting in intense multi-degree of freedom motion [1], [2]. Among them, roll motion [3], [4] poses the greatest threat to ships, quickly causing ship turbulence, and in severe cases, it can lead to ship sinking. Applying anti-roll fins [5], [6] has dramatically improved the anti-roll efficiency of ships. However, when encountering complex ocean obstacle fields, not only anti-roll measures need to be considered but also obstacle avoidance of the fin body needs to be considered to avoid damage to the fins, which may lead to a decrease in the system's anti-roll efficiency or even complete loss of function. Therefore, achieving real-time obstacle avoidance of fin stabilisers while meeting the requirements of system roll reduction has become an urgent challenge to be solved.

In recent years, the control theory in the marine field [7], [8] has developed rapidly. Given the uncertainty of the unknown structure of the ship and the nonlinear problems of the rolling model, many scholars have begun to try to improve the control performance of the system by using adaptive control [9]–[11], sliding mode control [12]–[14], and other methods. Reference [12] achieved error convergence by solving parameters and used the sliding mode inversion method to stabilise the system. Reference [13] considered the uncertainty problems, such as limited measurement, various disturbances, and changeable models. Reference [14] improved the fin shaft structure and used bearing deformation to solve force based on the nonlinear and uncertain characteristics of nonlinear roll motion model of a ship. Reference [11] proposed a robust adaptive fin stabiliser control algorithm based on L2 gain to address the nonlinear and uncertain issues of ships during turning, to reduce the swaying motion of the vessel after turning. With the development of artificial intelligence, more and more scholars find that if the powerful nonlinear fitting and mapping capabilities of neural networks are combined with control theory, the adaptability, and anti-interference of the system can be significantly improved [15]–[18]. Reference [15] separated the input and output of the system through a master–slave controller. Reference [16] adopted the Lyapunov function and adaptive control method to solve the issues of output limitation and unknown parameters. Reference [17] used a prediction algorithm based on radial basis function neural networks (RBF) to predict the roll motion of ships, thereby estimating the disturbance torque and roll time series. Then, a genetic algorithm-based inversion method was used to design a ship's roll control algorithm. Reference [18] solved the unknown sideslip

* School of Automation, Harbin University of Science and Technology, No.52 Xuefu Road, Nangang District, Harbin,, Heilongjiang, China 150080; e-mail: sunmingxiao@hrbust.edu.cn, 3462925679@qq.com, luantiantian@hrbust.edu.cn

** Key Laboratory of Advanced Manufacturing and Intelligent Technology, Ministry of Education, Harbin University of Science and Technology, No.52 Xuefu Road, Nangang District, Harbin, Heilongjiang, China 150080; e-mail: zhangyd1103@163.com
Corresponding author: Yongde Zhang

(DOI: 10.2316/J.2024.206-0789)

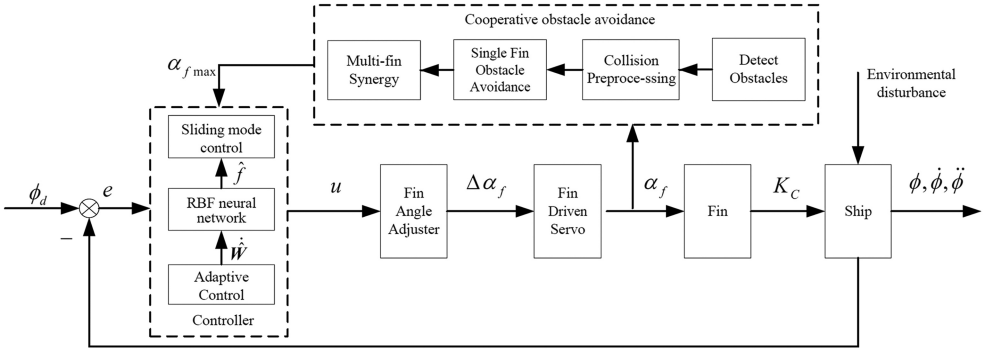

Figure 1. Block diagram of fin stabiliser cooperative obstacle avoidance control system.

angle of the vessel by using the radial basis function neural network. The above methods improve the control system's accuracy, fault tolerance, response speed, and anti-interference. But they did not consider the obstacle avoidance problem of anti-roll fin stabilisers.

When the stabiliser fin passes through an obstacle field, the controller should plan a safe working area for the fin body and consider the loss of stabiliser torque caused by the fin when avoiding obstacles. Considering the above problems, this work designs an obstacle avoidance control algorithm for the stabiliser fin, which ensures the safety of the stabiliser fin when passing through complex ocean obstacle fields as much as possible. Combining it with the adaptive RBF neural network-based collaborative control algorithm for the stabiliser fin not only compensates for the nonlinearity and uncertainty of the model but also avoids the problem of reduced stabilisation efficiency when the stabiliser fin avoids obstacles. Finally, the rationality and effectiveness of the fin stabiliser controller were verified through simulation.

2. Nonlinear Roll Motion Model of Ships

The roll motion model of the ship under strong external disturbance is with strong nonlinearity. The nonlinear roll motion model of the boat without fin stabilisers [19] is

$$\begin{aligned}(I_x+\Delta I_x)\,\ddot{\phi}+B_1\dot{\phi}+B_2\left|\dot{\phi}\right|\dot{\phi}\\ +C_1\phi+C_2\phi^3+C_3\phi^5=-Dh\alpha_m\end{aligned}\tag{1}$$

where B_1, B_2, C_2, and C_3 are the constants related to the ship. C_1 is the product of ship displacement and initial metacentric height, I_x is the moment of inertia of the hull, ΔI_x is the additional moment of inertia, ϕ is the roll angle, D is the ship displacement, h is the initial metacentric height of the ship, α_m is the effective wave slope.

The control torque [20] provided by a single fin is

$$K_C=\frac{1}{2}\rho v^2 A_f C_L^{\alpha}\left(\alpha_f+\frac{\dot{\phi}l_f}{v}\right)l_f\tag{2}$$

where ρ is the density of seawater, v is the relative velocity between the ship's speed and the ocean current, approximately taken as the ship's speed in engineering practice, A_f is the area of the fin stabiliser, C_L^{α} is the lift coefficient of the fin stabiliser, α_f is the effective angle of attack for the fin stabiliser and the incoming flow, l_f is the moment arm for the fin stabiliser.

The nonlinear roll motion model of a ship equipped with two pairs of fin stabilisers is

$$\begin{aligned}(I_x+\Delta I_x)\,\ddot{\phi}+B_1\dot{\phi}+B_2\left|\dot{\phi}\right|\dot{\phi}+C_1\phi+C_2\phi^3+C_3\phi^5\\ =-Dh\alpha_m-2\rho v^2 A_f C_L^{\alpha}\left(\alpha_f+\frac{\dot{\phi}l_f}{v}\right)l_f\end{aligned}\tag{3}$$

When the control torque $4K_C$ provided by the two pairs of fin stabilisers cancels out the roll torque $\mathrm{Dh}\alpha_m$, the ship's rolling motion will stop.

3. Design of the Controller for Collaborative Obstacle Avoidance of Fin Stabiliser

Due to the changeable interference from external and the uncertainty of (3) exists, this work uses an adaptive RBF neural network to approximate its uncertain term and design network weights and consider the influence of the ship roll angle change on the anti-rolling efficiency when the fin stabiliser system avoids obstacles. The block diagram of the fin stabiliser cooperative obstacle avoidance control system is shown in Fig. 1.

The primary purpose of the fin stabiliser system is to control the roll angle ϕ of the ship to approach zero. Among Fig. 1, ϕ_d is the expected output roll angle, the expected value of which is 0, e is the tracking error of the fin stabiliser system, α_{fmax} is the maximum fin angle allowed by the obstacle avoidance fin during obstacle avoidance, u is a fin stabiliser adaptive RBF neural network cooperative obstacle avoidance control ratio, $\widehat{f}$ is the RBF network output, $\widehat{W}$ is the adaptive rate, $\Delta\alpha_f$ is the fin angle that needs to be changed for obstacle avoidance, and meeting $\varepsilon_M \geq |\Delta\alpha_f|$, ε_M is constant.

3.1 Adaptive RBF Neural Network Control

According to (3), assumption $x_1=\phi$, $\dot{x}_1=x_2$, $y=x_1$, that is x_1 and x_2 are the ship's roll angle and roll angular velocity, respectively, y is the output of the fin stabiliser system. The nonlinear state space expression of ship roll

can be obtained as

$$\begin{cases} \dot{x}_1 = x_2 \\ \dot{x}_2 = a_1 x_1 \ + a_2 x_1^3 + a_3 x_1^5 + a_4 x_2 \\ \qquad\quad + a_5 x_2 \cdot |x_2| + a_6 \alpha_m + a_7 \alpha_f \\ y = x_1 \end{cases} \tag{4}$$

where parameters a_1, a_2, a_3, a_4, a_5, a_6 and a_7 is the coefficient obtained by transforming (3) into (4).

$f(x)$ represents the change of the uncertainty parameter of the roll motion model, assumption $f_0(x) = a_1 x_1 \ + a_2 x_1^3 + a_3 x_1^5 + a_4 x_2 \ + a_5 x_2 \cdot |x_2|$, then from (4), the following can be obtained:

$$\begin{cases} \dot{x}_1 = x_2 \\ \dot{x}_2 = f_0(x) + f(x) + b_0 u + d(t) \\ y = x_1 \end{cases} \tag{5}$$

where $b_0 = a_7$, $u = \alpha_f$, $d(t) = a_6 \alpha_m$, and $d(t) \le D_0$, D_0 is a constant representing the upper bound of the error.

From Fig. 1, the tracking error of the system is

$$e = \phi_d - \phi = -x_1 \tag{6}$$

The sliding mode function design is $s = \dot{e} + ce$ and $c > 0$, so

$$\begin{aligned} \dot{s} &= \ddot{e} + c\dot{e} = \ddot{\phi}_d - \ddot{\phi} + c\dot{e} = \ddot{\phi}_d - \ddot{x}_1 + c\dot{e} \\ &= \ddot{\phi}_d - f_0 - f - b_0 u - d(t) + c\dot{e} \end{aligned} \tag{7}$$

The sliding mode control law of the fin stabiliser system that can be designed is

$$\alpha_f = \frac{\left(-f_0 - f + \ddot{\phi}_d + c\dot{e} + \eta sgn(s)\right)}{b_0} \tag{8}$$

Substituting (8) into (7), the following will be got

$$\dot{s} = \ddot{\phi}_d - f_0 - f - b_0 u - d(t) + c\dot{e} = -\eta sgn(s) - d(t) \tag{9}$$

where η is the gain of the switch item.

If $\eta \ge 0$, the following will be got

$$s\dot{s} = s\left(-\eta sgn(s) - d(t)\right) = -\eta |s| - s \cdot d(t) \le 0 \tag{10}$$

x is the input of the RBF network. Then, the output is

$$\widehat{f}(x) = \widehat{W}^T h(x) \tag{11}$$

where $\widehat{W}$ is the estimated weight of the RBF network, $h(x)$ is the Gaussian function of RBF network, $\widehat{f}(x)$ is used to approximate $f(x)$.

Through (8), the control law of the fin stabiliser system can be obtained, and the fin angle is

$$\alpha_f = \frac{\left(-f_0 - \widehat{f} + \ddot{\phi}_d + c\dot{e} + \eta sgn(s)\right)}{b_0} \tag{12}$$

From the (12), the convergence speed of the control system depends on the control parameters c and η. Although, in theory, the larger the parameter c, the faster the error convergence speed of the system. In practice, if the parameter c is too large, it will cause the action speed and amplitude of the stabiliser to be too large, easily exceeding the execution limit of the stabiliser and damaging the stabiliser. Similarly, the larger the parameter η, the faster the convergence speed of the control system. However, if parameter η is too large, it can cause serious chattering in the anti-roll fin control system and exacerbate the wear of the anti-roll fin mechanism. Therefore, the size of these parameters should be reasonably selected. After multiple simulations and verifications, the control parameters c and η suitable for this work are 15 and 12.

3.2 Adaptive RBF Neural Network Obstacle Avoidance Control

When a fin avoids obstacles, it must change its angle and inevitably lose part of the control torque, reducing the anti-rolling efficiency. Using the real-time obstacle avoidance method of fin stabiliser, the maximum allowable angle of the fin body to safely avoid obstacles is solved α_{fmax}. Including the following specific steps:

Step 1: If the fin stabiliser crashes with an obstacle, obtain the overall equivalent model of the fin stabiliser for real-time obstacle avoidance and the front view analysis diagram, as shown in Fig. 2.

Figure 2(a) is the overall equivalent model of a fin stabiliser for real-time obstacle avoidance. In the equivalent sphere model, the obstacle is equivalent to the particle P and is the sphere's centre. The radius R of the particle P is the equivalent safety distance between the particle P and the fin body, size of R correlates with it. When the fin body is parallel with the horizontal plane, the longest horizontal length, vertical length, and vertical length of the fin body are, respectively, equivalent to the length d, width l, and height H of the cuboid, and then obtain an equivalent model cuboid of the fin body. The centre point of the fin axis 1 in the fin body is marked as point O. The model's centre point of the right face 2 is marked as point Q. The projection of point O on the plane where the rear side 3 of the model is marked as point B. The projection of point Q on the plane of the back side 2 is marked as point C.

Figure 2(b) is the overall front view analysis diagram of the real-time obstacle avoidance of the fin stabiliser, that is, the front view analysis diagram of Fig. 2(a). The vertical foot point of the particle P on the X axis is marked as point E, and the intersection point of the vertical line and the arc is marked as point F.

Step 2: Figure 2(a), φ_1, φ_2 are the values of $\angle OBP$ and $\angle QCP$, respectively, at this time φ_1 and φ_2 are

$$\begin{cases} \varphi_1 = \arccos \frac{\left(m^2 + (0.5l)^2 - x^2\right)}{(m \cdot l)} \\ \varphi_2 = \arccos \frac{\left(n^2 + (0.5l)^2 - y^2\right)}{(n \cdot l)} \end{cases} \tag{13}$$

where m is the distance of straight line BP, n is the distance of straight line CP, x is the distance of straight line OP, y is the distance of straight line QP.

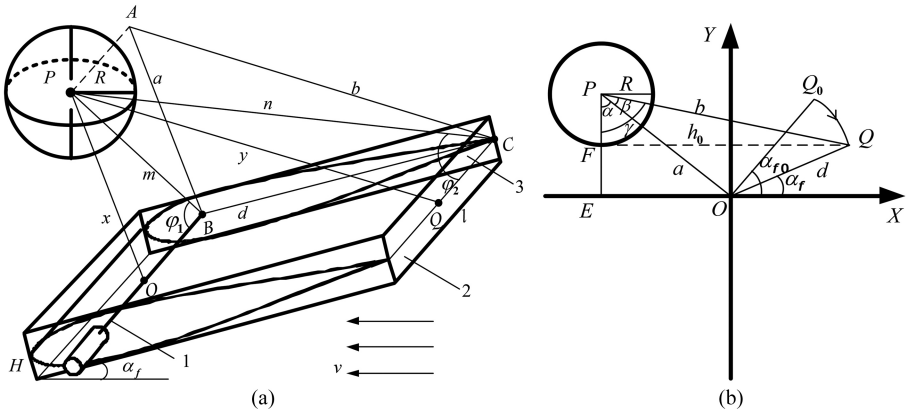

Figure 2. The overall equivalent model and main view analysis of the real-time obstacle avoidance of the fin stabilizer: (a) equivalent model and (b) analysis chart of main view.

Step 3: Figure 2(b), β and γ are the values of $\angle OPQ$ and $\angle EPQ$, respectively, at this time β and γ are

$$\begin{cases} \beta = \arccos\left(\frac{\left(a^2+b^2-d^2\right)}{(2a\cdot b)}\right) \\ \gamma = \arcsin\left(\frac{h_0}{b}\right) \end{cases} \tag{14}$$

where a is the distance of straight line OP, and it satisfies the equation $\frac{a\cdot l}{4} = \left(\frac{m\cdot l}{4}\right)\cdot\sin\varphi_1$. b is the distance of straight line QP, and it satisfies the equation $\frac{b\cdot l}{4} = \left(\frac{n\cdot l}{4}\right)\cdot\sin\varphi_2$. h_0 is the distance of straight line QF, and it satisfies the equation $h_0^2 + R^2 = b^2$.

Step 4: Combine with Fig. 2(b) shows that α_{fmax} and $\Delta\alpha_f$ are

$$\begin{cases} \alpha_{\text{fmax}} = \arcsin\left(\frac{(a\cos\alpha - R)}{d}\right) \\ \Delta\alpha_f = \alpha_{\text{fmax}} - \alpha_{f0} \end{cases} \tag{15}$$

where α is the value of $\angle EPO$, and the relationship of γ and β satisfies $\alpha = \gamma - \beta$, α_{f0} is the initial angle between the horizontal plane and the fin body when avoiding obstacles.

According to the above steps, α_{fmax} and $\Delta\alpha_f$ can be obtained, the safe area of the fin body is

$$\begin{cases} \alpha_{\text{fmax}} \geq \alpha_f \ \ \alpha_f > 0 \\ \alpha_{\text{fmax}} \leq \alpha_f \ \ \alpha_f < 0 \end{cases} \tag{16}$$

When single-fin obstacle avoidance, (3) can be rewritten as

$$\begin{aligned} &\left(I_x + \Delta I_x\right)\ddot{\phi} + B_1\dot{\phi} + B_2\left|\dot{\phi}\right|\dot{\phi} + C_1\phi + C_2\phi^3 + C_3\phi^5 \\ &\quad = -Dh\alpha_m - \left(2K_{C1} + 2K_{C2}\right) \end{aligned} \tag{17}$$

where K_{C1} is the front fin control torque during obstacle avoidance, and satisfies the formula $K_{C1} = \frac{1}{2}\rho v^2 A_f C_L^{\alpha}\left(\alpha_f + \Delta\alpha_f + \frac{\dot{\phi} l_f}{v}\right) l_f$, K_{C2} is the rear fin control torque, and satisfies the equation $K_{C2} = \frac{1}{2}\rho v^2 A_f C_L^{\alpha}\left(\alpha_f + \frac{\dot{\phi} l_f}{v}\right) l_f$.

According to the above combine with (12), the obstacle avoidance control law of the fin stabiliser system is

$$u = \frac{\left(-f_0 - \widehat{f} + \ddot{\phi}_d + c\dot{e} + \eta sgn\left(s\right)\right)}{b_0} - \Delta\alpha_f \tag{18}$$

3.3 Adaptive RBF Neural Network Cooperative Obstacle Avoidance Control Law Design

Substituting (18) into (9) can get

$$\dot{s} = -f + \widehat{f} - d\left(t\right) - \eta sgn\left(s\right) + \Delta\alpha_f \tag{19}$$

According to the RBF network algorithm, it can be known

$$\begin{cases} h_j = e^{\frac{\left\|x - c_{\text{ij}}\right\|^2}{\left(2b_j^2\right)}} \\ f = W^{*T} h\left(x\right) + \varepsilon \end{cases} \tag{20}$$

where the network input is x, the number of nodes is i, the number of nodes in the hidden layer is j, and h_j is the output of the Gaussian kernel function in the hidden layer. b_j is the base width vector of the neurons in the hidden layer, and the larger its value, the stronger the network's mapping ability to the input. If b_j is too small, it may cause the network to ignore the impact of some inputs on the network, but too large may cause the network to ignore the differences between inputs, resulting in poor performance. So b_j should is set to a moderate value. Similarly, c_{ij} is the centre coordinate vector of the neurons, and the closer the network input is to the coordinates, the more sensitive the Gaussian kernel function is to the input. c_{ij} should make the Gaussian kernel function within the effective input mapping range, the parameter W^* is the expected weight, the parameter ε is the approximation error, and it satisfies $|\varepsilon| \leq \varepsilon_N$.

If $\widetilde{f} = f - \widehat{f}$, $\widetilde{W} = W^* - \widehat{W}$, combining (19) and (20), the following will be obtained:

$$\begin{aligned} \dot{s} &= -\widetilde{f} - d\left(t\right) - \eta sgn\left(s\right) + \Delta\alpha_f \\ &= -\widetilde{W}^T h\left(x\right) - \varepsilon - d\left(t\right) - \eta sgn\left(s\right) + \Delta\alpha_f \end{aligned} \tag{21}$$

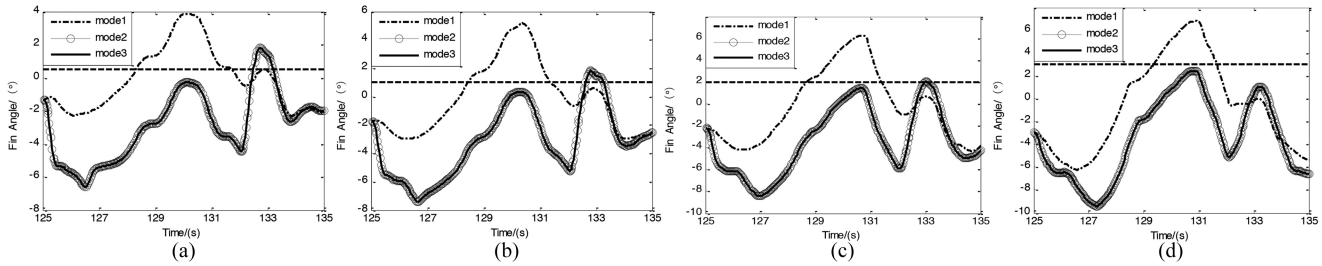

Figure 3. The fin angle changes of obstacle avoidance fins under different conditions: (a) $R = 0.15$ m; (b) $R = 0.25$ m; (c) $R = 0.35$ m; and (d) $R = 0.40$ m.

If $\gamma > 0$, and suppose the Lyapunov function is

$$V = 0.5s^2 + 0.5\gamma\widetilde{W}^T\widetilde{W} \tag{22}$$

Combining (21) and (22), the following can be got

$$\begin{aligned}\dot{V} &= -\widetilde{W}^T\left(sh\left(x\right) + \gamma\dot{\widehat{W}}\right) \\ &\quad -s\left(\varepsilon + d\left(t\right) + \eta sgn\left(s\right) - \Delta\alpha_f\right)\end{aligned} \tag{23}$$

From (23), the adaptive rate can be obtained as

$$\dot{\widehat{W}} = -\frac{sh\left(x\right)}{\gamma} \tag{24}$$

Combining (23) and (24), the following can be got

$$\begin{aligned}\dot{V} &= -s\left(\varepsilon + d\left(t\right) + \eta sgn\left(s\right) - \Delta\alpha_f\right) \\ &= -s\left(\varepsilon + d\left(t\right) - \Delta\alpha_f\right) - \eta\left|s\right|\end{aligned} \tag{25}$$

Because ε can take any small value so that $\eta \geq \varepsilon_N + \varepsilon_M + D_0$, therefore $\dot{V} \leq 0$. When $\dot{V} \equiv 0$, $s \equiv 0$, according to the LaSalle invariance theorem, it can be known that the fin stabiliser control system is gradually stable, when $t \to \infty$, there is $s \to 0$. Because $V \geq 0$, $\dot{V} \leq 0$, there is $t \to \infty$, V is bounded, so it proved that $\widehat{W}$ is bounded.

To avoid chattering in the control system as much as possible, the concepts of "boundary layer" and "quasi sliding mode control" are introduced in this work, which means the function $\mathrm{sat}\left(s\right)$ is used instead of the function $\mathrm{sgn}\left(s\right)$. After several simulation tests, this paper's optimal boundary layer thickness is 1.20, and the function $\mathrm{sat}\left(s\right)$ is

$$\mathrm{sat}\left(s\right) = \begin{cases} 1 & s > \Delta \\ \mathrm{ks} & \left|s\right| \leq \Delta, k = 1/\Delta \\ -1 & s < -\Delta \end{cases} \tag{26}$$

where Δ is the thickness of the boundary layer.

From (17), the part of the control torque will be reduced during obstacle avoidance, resulting in the fluctuation of ship roll angle. The cooperative control of the front and rear fin compensates for the reduced control torque. After compensation, the (17) can be rewritten as

$$\begin{aligned}&\left(I_x + \Delta I_x\right)\ddot{\phi} + B_1\dot{\phi} + B_2\left|\dot{\phi}\right|\dot{\phi} + C_1\phi + C_2\phi^3 + C_3\phi^5 \\ &\quad = -Dh\alpha_m - \left(2K'_{C1} + 2K'_{C2}\right)\end{aligned} \tag{27}$$

where K'_{C1} is the front fin control torque when the fin stabiliser cooperates with obstacle avoidance, and satisfied $K'_{C1} = K_{C1}$, K'_{C2} is the rear fin control torque when the fin stabiliser cooperates with obstacle avoidance, and it satisfies the equation $K'_{C2} = \frac{1}{2}\rho v^2 A_f C_L^{\alpha}\left(\alpha_f - \Delta\alpha_f + \frac{\dot{\phi} l_f}{v}\right) l_f$.

From (27), the coordinated control of the front and rear fins can compensate for the reduced roll stabilisation efficiency due to obstacle avoidance.

4. Simulation Study

A simulation study of the fin stabiliser system is carried out to verify the feasibility and effectiveness of the cooperative obstacle avoidance controller. The relevant parameters [18] of the selected ship type are displacement $D = 1.4573 \times 10^6$ kg, metacentric height $h = 1.15$ m, $I_x + \Delta I_x = 3.4383 \times 10^6$, $C_1 = Dh$, $C_2 = 2.097 \times 10^6$, $C_3 = 4.814 \times 10^6$, $B_1 = 0.636 \times 10^6$, $B_2 = 0.790 \times 10^6$. And the selected fin parameters are chord length $l = 2.49$ m, and the fin shaft is located 1/5 from the first edge. The initial state of the fin stabiliser cooperative obstacle avoidance control system is [0.2 0]. The uncertainty parameter of the roll model is taken $f\left(x\right) = 0.02\sin\left(t\right)$, and the adaptive parameter γ is 0.40. The structure of the RBF neural network is 2-5-1, and since the centre coordinates and the base width of the Gaussian kernel function should be selected according to the input range of the neural network in the simulation, the parameters c_{ij} and b_j are set to $[-1.0\ -0.5\ 0\ 0.5\ 1.0]$ and 1.0, respectively. Initial weight is 0.0.

When the front of the fin is about to encounter obstacles with equivalent ball radius of 0.15 m, 0.25 m, 0.35 m, and 0.40 m, the fin angle change of the obstacle avoidance fin is shown in Fig. 3.

In Fig. 3, mode1, mode2, and mode3 are, respectively, traditional RBF control, obstacle avoidance control, and cooperative obstacle avoidance. From Fig. 3(a)–(d), it is known that when the obstacle avoidance starts at 125 s, the fin angle change command is issued to start obstacle avoidance. When obstacle avoidance ends for 132 s, that is cancel the fin angle change command and resume normal operation. The horizontal dashed line in Fig. 3 is the value of the maximum obstacle avoidance fin angle α_{fmax}, indicates the maximum fin angle allowed to change when avoiding obstacles. When the range of Fig. 3(a)–(d) at 125 s $\sim$ 132 s, the corresponding maximum fin angles are 3.8772°, 5.1697°, 6.2583°, 6.8152°, respectively. Obstacle avoidance control and coordinated obstacle avoidance are controls when considering obstacle avoidance, when Fig. 3(a)–(d) at 125 s $\sim$ 132 s, the

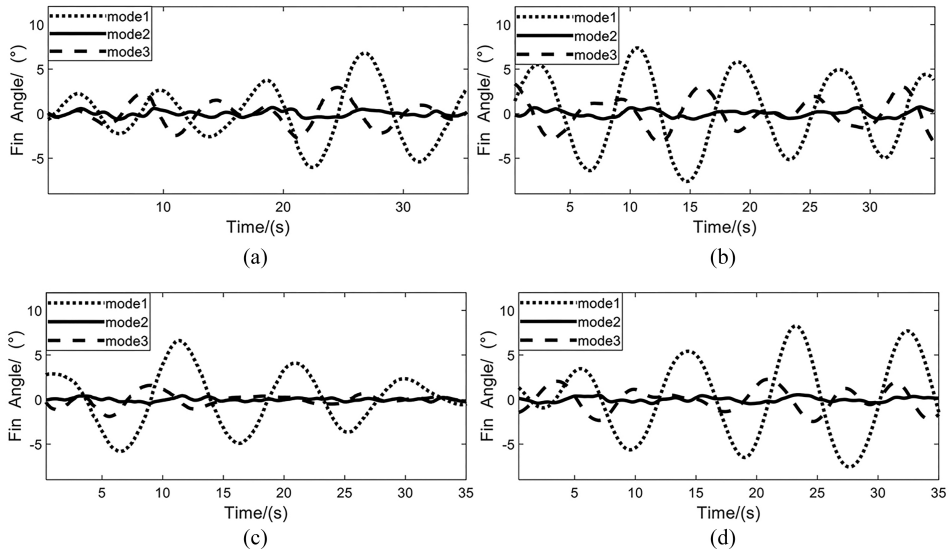

Figure 4. Change of ship roll angle with different controllers at various speeds: (a) $v = 9$ kn; (b) $v = 12$ kn; (c) $v = 15$ kn; and (d) $v = 18$ kn.

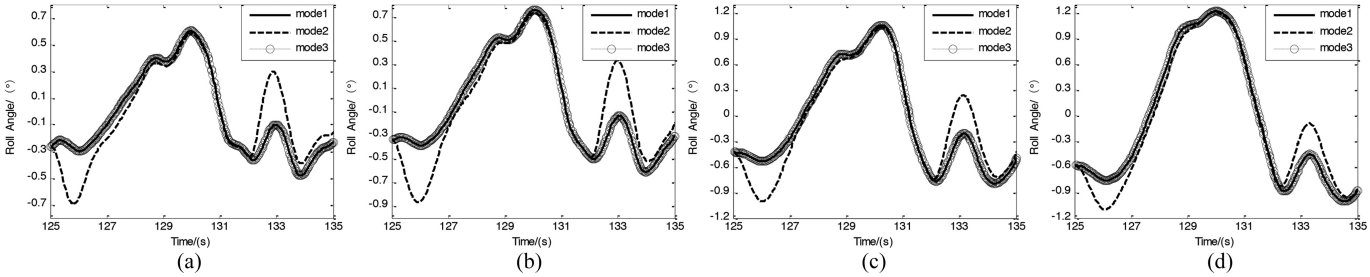

Figure 5. Change of ship roll angle under different conditions: (a) $\alpha_{\text{fmax}} = 0.5°$; (b) $\alpha_{\text{fmax}} = 1°$; (c) $\alpha_{\text{fmax}} = 2°$; and (d) $\alpha_{\text{fmax}} = 3°$.

corresponding maximum fin angle is $-0.2790°$, $0.3404°$, $1.4453°$, $2.4490°$.

When the ship does not encounter obstacles at different speeds, the effects of different anti-roll controllers are shown in Fig. 4. In Fig. 4, mode1, mode2, and mode3 are none-fin, cooperative obstacle avoidance controller, and PID controller.

From Fig. 4(a)–4(d), it can be seen that at speeds of 9, 12, 15, and 18 knots, the maximum roll reduction efficiency of the PID controller was 48%, 61%, 67% and 72%, respectively, while the maximum roll reduction efficiency of the cooperative obstacle avoidance controller was 92.0%, 93.3%, 93.7% and 95.1%, respectively.

According to (15), when the front of the fin is about to encounter obstacles with equivalent ball radius of 0.15 m, 0.25 m, 0.35 m, and 0.40 m, the maximum fin angle of obstacle avoidance is 0.5°, 1°, 2°, 3°, the roll angle of the ship changes as shown in Fig. 5.

In Fig. 5, mode1, mode2, and mode3 are, respectively, traditional RBF control, obstacle avoidance control, and cooperative obstacle avoidance. In the figure, the obstacle avoidance process and Fig. 3 occur in 125 s $\sim$ 132 s. From Fig. 5(a)–(d), it can be seen that the obstacle avoidance control fluctuates greatly in 125 s $\sim$ 127 s at the beginning of obstacle avoidance and 132 s $\sim$ 134 s after the end of obstacle avoidance, and the change trend of cooperative obstacle avoidance is basically the same as the change trend of traditional RBF control roll angle.

In the case of Fig. 5(a)–(d), 125 s $\sim$ 127 s at the beginning of obstacle avoidance. Compared with the obstacle avoidance control, the absolute value of the maximum roll angle fluctuation of the cooperative obstacle avoidance is increased by 1.55 times, 8.37 times, 1.17 times, and 0.66 times, respectively. However, 132 s $\sim$ 134 s after the end of obstacle avoidance, compared with the coordinated obstacle avoidance, the absolute value of the maximum roll angle fluctuation of the obstacle avoidance control, increased by 0.87 times, 0.80 times, 0.69 times, and 0.69 times, respectively.

The roll angle of obstacle avoidance control varies approximately linearly with time in 125 s $\sim$ 126 s, 126 s $\sim$ 127 s, 132 s $\sim$ 133 s, 133 s $\sim$ 134 s. In the figure, the changes of 125 s $\sim$ 126 s and 126 s $\sim$ 127 s, 132 s $\sim$ 133 s, and 133 s $\sim$ 134 s show a symmetrical feature. For the convenience of statistics, data analysis and statistics are only performed on the anti-rolling efficiency of 125 s $\sim$ 126 s, 132 s $\sim$ 133 s. The data are shown in Tables 1 and 2.

Table 1
Statistics of Anti-Rolling Data at the Beginning of Obstacle Avoidance

v/kn	Obstacle avoidance control	Maximum fin angle for obstacle avoidance (°)					
		0.5	1	1.5	2	2.5	**3**
8	Standard deviation of roll angle Anti-rolling efficiency	0.1090° 94.96%	0.1058° 95.10%	0.1042° 95.18%	0.1011° 95.32%	0.0981° 95.46%	0.0966° 95.53%
10	Standard deviation of roll angle Anti-rolling efficiency	0.1284° 94.06%	0.1247° 94.23%	0.1198° 94.50%	0.1101° 94.91%	0.1047° 95.16%	0.0961° 95.55%
12	Standard deviation of roll angle Anti-rolling efficiency	0.2594° 88.00%	0.2397° 88.91%	0.2259° 89.55%	0.2181° 89.91%	0.2025° 90.63%	0.1853° 91.43%
14	Standard deviation of roll angle Anti-rolling efficiency	0.2796° 87.06%	0.2551° 88.20%	0.2382° 88.98%	0.2177° 89.92%	0.2018° 90.66%	0.1795° 91.69%
16	Standard deviation of roll angle Anti-rolling efficiency	0.2447° 88.68%	0.2137° 90.11%	0.1836° 91.50%	0.1566° 92.75%	0.1356° 93.72%	0.1124° 94.80%
18	Standard deviation of roll angle Anti-rolling efficiency	0.1775° 91.79%	0.1506° 93.03%	0.1296° 94.00%	0.1029° 95.24%	0.0803° 96.28%	0.0598° 97.23%

Table 2
Statistics of Anti-Rolling Data After Obstacle Avoidance

v/kn	Obstacle avoidance control	Maximum fin angle for obstacle avoidance (°)					
		0.5	1	1.5	2	2.5	**3**
8	Standard deviation of roll angle Anti-rolling efficiency	0.3169° 74.81%	0.3165° 74.84%	0.3162° 74.86%	0.3156° 74.91%	0.3148° 74.98%	0.3143° 75.02%
10	Standard deviation of roll angle Anti-rolling efficiency	0.4274° 66.03%	0.4201° 66.61%	0.4167° 66.88%	0.4065° 67.69%	0.4008° 68.14%	0.3873° 69.21%
12	Standard deviation of roll angle Anti-rolling efficiency	0.2628° 79.11%	0.2528° 79.90%	0.2355° 81.28%	0.2225° 82.31%	0.2053° 83.68%	0.1884° 85.02%
14	Standard deviation of roll angle Anti-rolling efficiency	0.4117° 67.27%	0.3942° 68.66%	0.3743° 70.25%	0.3432° 72.72%	0.3269° 74.01%	0.3077° 75.54%
16	Standard deviation of roll angle Anti-rolling efficiency	0.3411° 72.89%	0.3179° 74.73%	0.2954° 76.52%	0.2692° 78.60%	0.2462° 80.43%	0.2251° 82.11%
18	Standard deviation of roll angle Anti-rolling efficiency	0.2606° 79.28%	0.2341° 81.39%	0.2130° 83.07%	0.1851° 85.29%	0.1629° 87.05%	0.1424° 88.68%

To further explore the relationship between the maximum obstacle avoidance fin angle and the anti-rolling efficiency. Tables 1 and 2 are fitted with the corresponding anti-rolling efficiency under different obstacle avoidance maximum fin angles and different speeds. As shown in Fig. 6.

It can be seen from Fig. 6. When the speed is 8 kn $\sim$ 18 kn and the maximum obstacle avoidance fin angle is 0.5° $\sim$ 3°, the maximum obstacle avoidance fin angle and the anti-rolling efficiency are approximately linearly positive. With the continuous increase of the maximum fin angle of obstacle avoidance, the anti-rolling efficiency is also increasing. Nevertheless, when the speed of 132 s $\sim$ 133 s is 8 kn after the end of obstacle avoidance, with the increase of the maximum fin angle of obstacle avoidance, the anti-rolling efficiency only increases by 0.21%.

5. Conclusion

The conclusions are as follows:

1) Considering the lack of real-time obstacle avoidance in traditional fin stabilisers, this work uses a collaborative obstacle avoidance control method to solve the maximum fin angle for obstacle avoidance. It plans the safe motion area of the fin body, thus achieving reasonable obstacle avoidance of the fin stabiliser.
2) Considering that the anti-roll fin may reduce the efficiency during obstacle avoidance, compensation was provided through the collaborative control of the front and rear fins, which met the system's anti-roll requirements while avoiding obstacles and solved the problem of reduced anti-roll efficiency during obstacle avoidance.

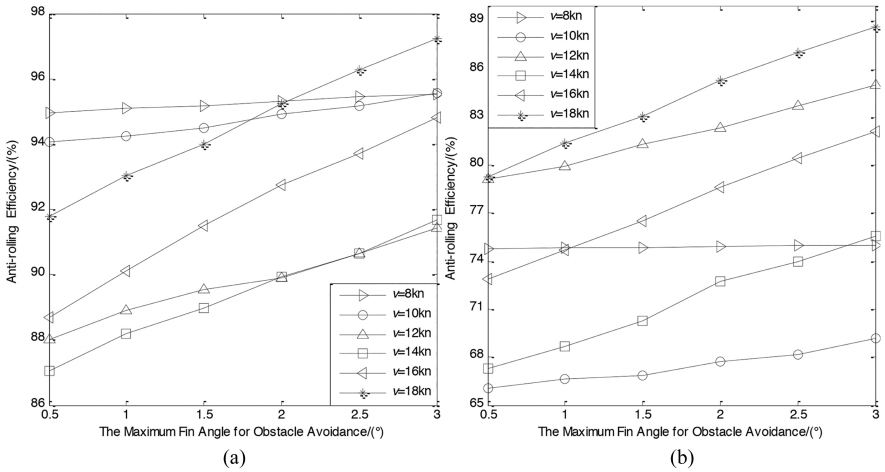

Figure 6. The relationship between the maximum fin angle of obstacle avoidance and the efficiency of anti-rolling: (a) obstacle avoidance begins (125 s $\sim$ 126 s) and (b) obstacle avoidance is over (132 s $\sim$ 133 s).

3) The problem of the significant drop in anti-rolling efficiency at the beginning and after the end of obstacle avoidance is explored. After the data of these two states are processed in sections, the maximum fin angle of obstacle avoidance and anti-rolling efficiency are approximately linearly positively correlated.

The next step is to study the special situation in which changing the fin angle cannot meet the requirements of fin obstacle avoidance, and further improve the fin stabiliser obstacle avoidance system.

Acknowledgement

This research was funded by the National Science Foundation for Young Scientists of China, grant number 62103120, the National Science Foundation for Heilongjiang Province, grant number LH2021F033, Heilongjiang Postdoctoral Grant, grant numbers LBH-Z22197 and LBH-Z22195, and Heilongjiang Provincial Technological Innovation Center of Efficient Molding of Composite Materials and Intelligent Equipment, grant number HPTIC202204.

Conflict of Interests

The authors declare no conflict of interests.

References

[1] J. Jiao, S. Huang, and C.G. Soares, Numerical investigation of ship motions in cross waves using CFD, *Ocean Engineering, 223*, 2021, 108711.

[2] Y.H. Wang, Y.L. Tuo, S.X. Yang, and M.Y. Fu, Nonlinear model predictive control of dynamic positioning of deep-sea ships with a unified model, *International Journal of Robotics and Automation, 31(6)*, 2016, 519–529.

[3] L. Hu, H. Wu, Z. Yuan, W. Li, and X. Wang, Roll motion response analysis of damaged ships in beam waves, *Ocean Engineering, 227*, 2021(2), 108558.

[4] D. Maalouf, V. Creuze, A. Chemori, and O. Tempier, Feedforward inertial actuation for roll stabilization of an underactuated underwater vehicle, *International Journal of Robotics and Automation, 30(1)*, 2015, 79–86.

[5] I.A. Jimoh, I.B. Küükdemiral, and G. Bevan, Fin control for ship roll motion stabilisation based on observer enhanced MPC with disturbance rate compensation, *Ocean Engineering, 224(4)*, 2021, 108706.

[6] L.H. Liang, M.X. Sun, H.Y. Shi, and T.T. Luan, Design and analyze a new measuring lift device for fin stabilizers using stiffness matrix of Euler-Bernoulli beam, *PLoS One, 12(1)*, 2017, 1–13.

[7] Z.X. Zhu, J.F. Zhong, M.Z. Ding, and M.M. Wang, Trajectory planning and hierarchical sliding-mode control of underactuated space robotic system, *International Journal of Robotics and Automation, 35(6)*, 2020, 436–443.

[8] M.X. Sun, T.T. Luan, L.H. Liang, and Y.W. Liu, Lift detection and analysis of fin stabilizers shaft based on Euler-Bernoulli stiffness matrix, *Journal of Ship Mechanics, 22(08)*, 2018, 944–954.

[9] L.H. Liang, M.X. Sun, and T.T. Luan, Design of adaptive control system for lift feedback of fin stabilizer, *Journal of Harbin Engineering University, 38(11)*, 2017, 1739–1744.

[10] C.C. Ku and C.Y. Hsu, Robust control of delayed fin stabilizer stochastic systems of a ship, *Proceedings of Engineering and Technology Innovation, 10*, 2018, 13–18.

[11] S.T. Zhang and P. Zhao, L2-gain based adaptive robust heel/roll reduction control using fin stabilizer during ship turns, *Journal of Marine Science and Engineering, 9(01)*, 2021, 89.

[12] Y.T. Zhang, W.R. Shi, and M.B. Qiu, Sliding backstepping control for fin stabilizer with nonlinear disturbance observer, *Control and Decision, 25(08)*, 2010, 1255–1260.

[13] M. Moradi and H. Malekizade, Robust adaptive first-second-order sliding mode control to stabilize the uncertain fin-roll dynamic, *Ocean Engineering, 69*, 2013, 18–23.

[14] L.H. Liang, M.X. Sun, and T.T. Luan, Design fuzzy input-based adaptive sliding mode control for vessel lift-feedback fin stabilizers with shock and vibration of waves, *Shock and Vibration, 2017*, 2017, 1–13.

[15] J.G. Song, L.H. Liang, H.Z. Jin, and Z.G. Qi, Adaptive master-slave controller for zero-speed fin stabilizer, *Control Theory and Applications, 32(05)*, 2015, 703–708.

[16] R.H. Li, T.S. Li, W.W. Bai, and X. Du, An adaptive neural network approach for ship roll stabilization via fin control, *Neurocomputing, 173*, 2016, 953–957.

[17] J.G. Song, L.H. Liang, S.T. Zhang, and J.M. Wang, Design and experimental investigation of a GA-based control strategy for a low-speed fin stabilizer, *Ocean Engineering, 218*, 2020, 108234.

[18] H.G. Zhang, X.K. Zhang, and R.X. Bu, Sliding mode adaptive control for ship path following with sideslip angle observer, *Ocean Engineering, 251*, 2022, 111106.

[19] M.X. Sun, T.T. Luan, and L.H. Liang, RBF neural network compensation-based adaptive control for lift-feedback system of ship fin stabilizers to improve anti-rolling effect, *Ocean Engineering, 163*, 2018, 307–321.

[20] W.R. Shi, F. Tao, and Y.T. Zhang, Adaptive sliding mode control for fin stabilizer based on RBF neural network, *Control Engineering of China, 19(06)*, 2012, 978–986.

Biographies

Mingxiao Sun received the B.E. and Ph.D. degrees from the College of Automation, Harbin Engineering University, Harbin, China, in 2010 and 2018, respectively. He is currently an Associate Professor with Harbin University of Science and Technology, Harbin, China. His research interests include ship motion control and robot.

Houxin Lian is currently an undergraduate student with Harbin University of Science and Technology, Harbin, China. His research interests include ship motion control and robot.

Yongde Zhang is currently a Professor with Harbin University of Science and Technology, Harbin, China. His research interests include ship motion control and robot.

Tiantian Luan received the B.E. and Ph.D. degrees from the College of Automation, Harbin Engineering University, Harbin, China, in 2011 and 2018, respectively. She is currently an Associate Professor with Harbin University of Science and Technology, Harbin, China. Her research interests include control science and engineering, robot, and decision support system.